

DNM3 modifies age of onset in LRRK2 parkinsonism: a linkage and association study

Joanne Trinh BSc^{1*}, Emil K Gustavsson MSc^{1,6}, Carles Vilariño-Güell PhD¹, Stephanie Bortnick BSc¹, Jeanne Latourelle PhD², Marna B McKenzie BSc¹, Chelsea Szu Tu MSc¹, Ekaterina Nosova PhD¹, Jaskaran Khinda BSc¹, Austen Milnerwood PhD¹, Suzanne Lesage PhD³, Alexis Brice MD⁴, Meriem Tazir MD PhD⁵, Jan Aasly MD PhD⁶, Laura Parkkinen PhD⁷, Hazal Haytural MSc⁷, Tatiana Foroud PhD⁸, Richard H Myers PhD⁹, Samia Ben Sassi MD¹⁰, Emna Hentati MD¹⁰, Fatma Nabli MD¹⁰, Emna Farhat MD¹⁰, Rim Amouri PhD¹⁰, Fayçal Hentati MD¹⁰ and Matthew J Farrer PhD¹

¹ Centre for Applied Neurogenetics, Department of Medical Genetics, 2215 Wesbrook Mall, University of British Columbia, Vancouver, BC, V6T 1Z3, Canada.

² Department of Neurology, Boston University School of Medicine, Boston, MA, USA.

³ Sorbonne Universités, UPMC Univ Paris 6 UMR S 1127, Inserm U 1127, CNRS UMR 7225, Institut du Cerveau et de la Moelle épinière, ICM, Paris, France

⁴ Sorbonne Universités, UPMC Univ Paris 6 UMR S 1127, Inserm U 1127, CNRS UMR 7225, Institut du Cerveau et de la Moelle épinière, ICM ; AP-HP, Hôpital de la Salpêtrière, Department of Genetics and Cytogenetics, Paris, France

⁵ Service de Neurologie CHU Mustapha, Alger, Algérie

⁶ Department of Neurology (J.A.), St Olav's Hospital, Trondheim, Norway

⁷ Nuffield Department of Clinical Neurosciences, University of Oxford, Oxford, UK.

⁸ Department of Medical and Molecular Genetics, Indiana University School of Medicine, Indianapolis, IN, USA.

⁹ Genome Science Institute, Boston University School of Medicine, Boston, MA, USA.

¹⁰ Mongi Ben Hamida National Institute of Neurology, La Rabta, Tunis, 1007, Tunisia.

* Corresponding Author:

¹ Department of Medical Genetics, University of British Columbia, Vancouver, BC, Canada, V6T 1Z3. Tel: (604) 822 7753. Fax: (604) 822-0361

E-mail: jtrinh@can.ubc.ca; mfarrer@can.ubc.ca

Text word count: 2582; Abstract: 276; Title Characters: 48; Figures: 3; Tables 1

References: 43; Supplementary tables: 10; Supplementary figures: 7

Running title: *DNM3* and *LRRK2* parkinsonism

Abstract

Background

LRRK2 c.6055G>A (p.G2019S) accounts for ~1% of Parkinson disease in Caucasians, 13-30% in Ashkenazi Jews and 30-40% in North-African Arab-Berbers, although age of onset (AOO) is variable; some carriers have early-onset parkinsonism while others remain asymptomatic despite an advanced age.

Methods

Patients with PD (age of the participants were ≥ 18 years) were recruited between 2006-2012 at the Mongi Ben Hamida National Institute of Neurology, Tunis. A diagnosis was made according to the UK Parkinson disease society brain bank criteria without exclusion of familial parkinsonism. AOO was assessed as a categorical (dichotomized by median onset) and quantitative trait. Genome-wide linkage analysis employed 41 multi-incident *LRRK2* p.G2019S Arab-Berber families (150 familial patients and 103 unaffected family members). Subsequent locus-specific genotyping and association analyses employed another 232 unrelated Tunisian *LRRK2* p.G2019S carriers. Whole-genome sequencing in a subset of 14 subjects informed imputation and haplotype analyses. Replication was sought in 263 *LRRK2* p.G2019S carriers originating from Algeria, France, Norway, and North America. Relationships between genotype, gene and protein expression were assessed in human control striatum and murine *LRRK2* p.G2019S cortical neurons.

Findings

Significant linkage was identified on chromosome 1q23·3-24·3 ($LOD_{NPL} = 2·9$ and model-based $LOD=4·99$, $\theta=0$ at D1S2768) in which association and haplotype mapping highlights genetic variability within *DNM3* as an AOO modifier of disease (rs2421947; haplotype $p=1·07 \times 10^{-7}$).

DNM3 rs2421947 is a haplotype-tag for which the median onset of *LRRK2* parkinsonism in GG carriers is 12.5 years younger than CC carriers (Tunisian series HR 1.89 CI=1.20-2.98).

Replication concurs although sample size was limited. *DNM3* expression varies as a function of rs2421947 genotype in human striatum and dynamin-3 localization is perturbed in murine *LRRK2* p.G2019S cortical neurons.

Interpretation

Genetic variability in *DNM3* modifies AOO for *LRRK2* p.G2019S parkinsonism and may inform disease pathophysiology, translational neuroscience and clinical trials design.

Funding

The Canada Excellence Research Chairs (CERC), Leading Edge Endowment Fund (LEEF), Don Rix BC Leadership Chair in Genetic Medicine, National Institute on Aging, National Institute of Neurological Disorders and Stroke, the Michael J Fox Foundation, Mayo Foundation, the Roger de Spoelberch Foundation and GlaxoSmithKline.

Introduction

Genetic variability in leucine-rich repeat kinase 2 (*LRRK2*) has been linked to familial parkinsonism and associated with idiopathic Parkinson disease (PD): *LRRK2* c.6055G>A (p.G2019S) confers the highest genotypic and population attributable risk.¹⁻³ Penetrance estimates are variable with a wide range in age of onset (AOO) influenced by ethnicity.⁴⁻⁶ The relatively homogeneous North-African Arab-Berber population has the highest frequency of *LRRK2* p.G2019S carriers, between 30-40% of patients with PD,^{7,8} and provides a unique opportunity to identify genetic modifiers of AOO.

LRRK2 is a large multi-domain protein with GTPase (Roc) and kinase activities that appear to modulate cytoskeletal outgrowth and vesicular dynamics including synaptic transmission⁹, endosomal trafficking and lysosomal autophagy.¹⁰ Although many binding partners and substrates have been identified it remains uncertain which are clinically relevant to disease pathophysiology. Herein, a genome-wide approach was used to identify genetic variability that directly influences *LRRK2* p.G2019S penetrance, albeit dichotomizing AOO about the median in our linkage discovery effort. The study reports a genetic association and a replication effort of a potential *LRRK2* AOO modifier.

Methods

Discovery and replication series

Arab-Berber subjects were recruited between 2006 to 2012 by movement disorders neurologists (FH, SBS, FN, EF) at the Mongi Ben Hamida National Institute of Neurology, Tunis. Community-based samples consisted of 41 multi-incident *LRRK2* p.G2019S families (150 affected and 103 unaffected *LRRK2* carriers) and 232 unrelated *LRRK2* p.G2019S carriers (Table 1a). All subjects were older than ≥ 18 years at neurological assessment and provided

informed consent prior to their participation. Specific approvals obtained from the local ethics committee at the National Institute and Ministry of Health in Tunis were reviewed by GlaxoSmithKline (GSK), the Institutional Review Board of Mayo Foundation and the Research Ethics Board of the University of British Columbia. Additional replication series included 263 LRRK2 p.G2019S carriers from Algeria (MT), France (AB), Norway (JAA), and North America (PSG–Progeni GenePD Investigators¹¹) (Table 1b). The mean age and age of onset is reported on Table 1b. The age-at-initial symptom was self-reported by patients whereas age-at-motor onset was assessed by the neurologist. The age-at-initial symptom onset was used as an outcome variable (AOO) in this study. Familial relationships were defined based on self-report. However, STR and SNP markers were used to test genetic relationships within Tunisian families. Human biological samples were sourced ethically and their research use was in accord with the terms of the informed consents. An overview of samples for discovery and replication is depicted in Figure 1.

Linkage analysis and STR genotyping

Genome wide linkage analysis was performed on 41 LRRK2 p.G2019S families from Tunisia using deCODE's 4cM density STR (short tandem repeat) marker set, with standard approaches.¹² Allele frequencies derived from Tunisian unrelated, non-carrier, control subjects were used for STRs. Consanguineous loops are noted in ~1/3rd of the families but were split to maximize information content.¹² Non-parametric (NPL) and model-based linkage analyses were performed using age at onset (AOO) as the trait. Model-based linkage used an additive model with incomplete penetrance to provide LOD (logarithm of odds) and hLOD (heterogeneity LOD) scores. As a categorical variable AOO was dichotomized by the median onset; we defined an early-onset group (all affected carriers with PD and an AOO <56 years) and a late-onset group

(all affected carriers with PD and an AOO ≥ 56 years and all unaffected carriers with an age at examination of ≥ 56 years). Alternatively, AOO in patients and age at recruitment/examination of unaffected carriers was assessed as a quantitative trait.

Genome-wide SNP genotyping and association

Single nucleotide polymorphisms (SNP) were genotyped for the Tunisian Arab-Berber cohort using Affymetrix 500K *NspI* and *StyI* (n=101) and Illumina Multi-Ethnic Genome Arrays (MEGA) (n=131). Affymetrix genotypes were extracted from .cel intensity files using three algorithms, BBRML, JAPL and CHIAMO, and only nominated when there was consensus, as previous¹³; GenomeStudio® was used to provide genotypes for Illumina data. Samples with genotype call rate below 99% were excluded from further analysis. Genotype distributions for all SNPs within all samples combined, all cases or control subjects, satisfied Hardy-Weinberg equilibrium (HWE) expectations ($p > 0.001$) (Text S1). PLINK was used to manage data and assess IBS, IBD and cryptic relatedness.¹⁴ Quantile-quantile plots of p-values were employed to highlight potential confounders (R package qqman). Population stratification was also assessed using Eigenstrat.¹⁵ Within regions of linkage (defined as NPL scores > 2.0 , with model-based LOD > 3.3) association analyses compared genotype counts between patients < 56 and ≥ 56 years at AOO (dichotomized by the median) using PLINK^{14, 16}. Alternatively, AOO was considered as a quantitative trait using Cox proportional hazards regression models, adjusting for gender and censoring at the age of last follow-up. Association analyses focused on SNPs within the maximum LOD -1 genomic intervals.

Whole genome sequencing and imputation

Whole genome sequencing (WGS) was accomplished for 14 Tunisian Arab-Berber LRRK2 p.G2019S carriers with a family history of parkinsonism; half had early-onset disease

(mean onset 34.9 years, $SD \pm 7.2$, range 22-42) and the remainder are clinically asymptomatic elderly carriers (mean age 77 years, $SD \pm 6.9$, range 68-90). Sequencing was carried out using Illumina 2x100 nucleotide paired-end reads, with minimum 50-fold mean depth using standard methods for sequence alignment, and variant calling (Figure S1).

SNP genotypes in significantly linked LOD -1 support intervals were imputed with Beagle 4.0,^{17, 18} employing 14 Tunisian WGS and phased 1000 Genomes data as a reference for Affymetrix and MEGA data (n=232 LRRK2 carriers). Within linked intervals haplotypes were subsequently defined by diallelic pseudomarkers using a variable-length Markov-chain Monte Carlo method.^{17, 18} As previous, AOO was dichotomized by the median as a categorical variable, and haplotypes were compared between patients <56 and ≥ 56 years at AOO, or assessed as a quantitative trait by linear regression, adjusting for gender. Empirical p-value estimates were determined by permutation testing (100,000 replicates).

Sequencing and genotyping

All subjects were screened for LRRK2 p.G2019S by Sanger sequencing or TaqMan SNP assays-on-demand (Life Technologies, Inc, Foster City, CA) and excluded for other pathogenic mutations implicated in PD.^{19, 20} Subsequent genotyping was carried out by a combination of Sequenom MassArray iPLEX system (Sequenom, San Diego, CA) and TaqMan genotyping. Cumulative incidence plots (Kaplan Meier) and hazard ratios (Cox proportional hazard regression models) were used to stratify age of initial symptom by genotypes using JMP® software (SAS Institute Inc., Cary, NC). These models were adjusted for family relatedness, gender and population series (Algeria, France, North America, Norway and Tunisia) (Table S10). Right censoring for asymptomatic carriers was performed at age of examination. Meta-analyses of all populations was performed with R-package 'metafor'.

Brains, RNA, Ampliseq Transcriptome, Antibodies

Brain tissue from 61 healthy control subjects without any neurological symptoms was obtained from the Oxford Brain Bank, University of Oxford (LP); any with neurodegenerative vascular pathology were excluded (LP). Full ethical approval (REC 07/Q2707/98) and written informed consent are obtained for all participants. Gender, age-at-death and *post mortem* delay was available for all subjects (Table S1). DNA was prepared from ~20mg of frozen tissue samples of striatum with an Autogen NA1000 and was quantified using standard methods. RNA, and protein were extracted as described (Text S1). Antibodies, primers and expression probes are as described (Text S1, Table S2, Figure S2). Prism 6.0 (GraphPad Software, Inc) was used for RNA/protein analysis. LRRK2 p.G2019S mice, primary neuronal littermate cultures, immunostaining and image analysis were as previously described.⁹

Role of the funding source

The funding sources had no role in study design, data collection, data analysis, data interpretation or writing of the report. All authors had full access to all the data in the study and had final responsibility for the decision to submit for publication.

Results

Linkage and association of LRRK2 p.G2019S families

Linkage analysis of AOO in 41 Tunisian LRRK2 p.G2019S pedigrees identified chromosome 12q12 using non-parametric ($LOD_{NPL}=3.3$, $\theta=0$ at D12S85) and model-based methods (maximum $LOD=7.6$, $\theta=0$ at D12S85 under a dominant model of inheritance), which encompasses the *LRRK2* locus. Genome-wide analysis using similar approaches, with allele-dependent penetrances, also identified chromosome 1q23.3-24.3 ($LOD_{NPL}=2.90$, maximum

LOD & hLOD = 4.99, $\theta=0$ at D1S2768 with a recessive model, and LOD=2.81 and hLOD=3.81, $\theta=0$ at D1S2768 with a dominant-additive model) (Figure 2a). Linkage analyses using AOO as a dichotomous trait were robust to subsequent ordered subset analyses over a range of divisions (Table S5).²¹ The highest LOD score across all models was obtained on chromosome 1q23.3-24.3 although significant scores were also obtained for chromosomes 17q25.3 and 21q21.2 (Figure S3).²¹

Evidence for association within the chromosome 1q23.3-24.3 linkage region (170.8-172.5Mb, the maximum LOD -1 support interval) was assessed in unrelated LRRK2 p.G2019S carriers (n=232). Association with dichotomized AOO revealed three associated SNPs (rs742510, rs2421947 and rs2206543, $r^2 = 0.98$; $p_{\text{nominal}} = 2.6 \times 10^{-5}$) within the dynamin-3 locus (*DNM3*) (Table S3a). While the QQ-plot for association analyses on chromosome 1 deviated from the line of equality the *DNM3* rs2421947 association was confirmed by TaqMan probe genotyping (Figure S4). AOO was also assessed as a quantitative trait using Cox regression modelling; *DNM3* was again the most significant finding (rs2421947, $p=0.0053$) albeit uncorrected for multiple testing. Interestingly, three other SNPs were nominated within chromosome 17 and 21 (rs4969113, rs986917 and rs382816) (Table S3b).

Subsequently, all 21 coding exons of *DNM3* gene were sequenced in LRRK2 p.G2019S carriers with extreme AOO including early-onset PD (<45 at onset, n=13) and elderly subjects without motor signs of PD (> 75years, n=12). Three rare synonymous variants were identified (p.A81A, p.H128H, and p.V609V; MAF<0.01).

Higher resolution mapping: Genome sequencing, imputation and haplotype analysis

WGS of 14 LRRK2 p.G2019S Tunisian Arab-Berber subjects and 1000 Genomes data provided references for SNP imputation, to improve haplotype analysis and identify specific variability associated with AOO. Within and flanking the *DNM3* locus (chr1:171,810,018-172,382,057) a dense framework of informative markers (MAF>0.05) was imputed in all unrelated LRRK2 carriers (n=232) with Affymetrix, MEGA and Sequenom iPLEX genotypes. The shortest, most significant haplotype associated with AOO was subsequently defined between chr1:171,832,491-171,833,094 (rs77565020 to rs2421947, 603bp), using variable-length Markov-chain Monte Carlo methods ($p=1.07 \times 10^{-7}$, Text S1), and remained significant after permutation analyses ($p=0.002$) (Figure 2b, Table S3c). The *DNM3* haplotype was also significantly associated when considering AOO as a continuous trait using a regression model ($p=0.00028$) (Table S3d). Another haplotype was nominated within the chromosome 17 linkage peak, albeit 30kb centromeric of the nearest gene, *LOC100134391* ($p=0.0007$). Other linkage regions did not show significant haplotype associations.

The Kaplan-Meier method was used to calculate median/IQR censoring at age of last examination for unaffected carriers by *DNM3* genotype. rs2421947 CC homozygous carriers had a median AOO of 64 years (IQR: 48-67); CG heterozygotes had a median 57 (IQR: 50.5-64 years) and GG homozygotes had a median 51.5 (IQR: 46-61.5 years) (Kaplan Meier log-rank p -value=0.03) (Figure 3a). The median onset of LRRK2 parkinsonism in *DNM3* rs2421947 GG homozygotes is 12.5 years younger than CC homozygotes. *DNM3* rs2421947 has a minor allele frequency (MAF) C= 0.42 in unrelated control subjects from Caucasian populations (HapMap-CEU, n=226) and 0.42 in unrelated control subjects from Tunisia (n=321). In LRRK2 p.G2019S carriers the MAF C=0.39 overall, irrespective of affection status, but increases to C=0.46 with disease onset ≥ 56 years (Table S6-9).

To fully estimate the effect of *DNM3* rs2421947 in the Tunisian population we combined the unrelated individuals and families in a Cox proportional hazard model, censoring unaffected individuals, while adjusting for family relatedness and gender (HR 1.63, CI=1.05-2.63, p=0.03 for alternate homozygous genotypes).

DNM3 expression

DNM3 rs2421947 was genotyped in striatal brain tissue (n=61) to assess any influence on expression. The rs2421947 GG genotype was correlated with higher *DNM3* mRNA levels (r=0.25, p=0.006) (Figure S5), with a 1.25-fold increase for the GG genotype compared to CC. Results were confirmed using Ampliseq whole transcriptome analysis in a subset of samples with alternate homozygous genotypes (n=17; transcriptome data available on request). The findings were robust to normalization with a variety of housekeeping genes (Text S1). *DNM3* total transcript expression was correlated with *LRRK2* ($r^2=0.65$ p=0.004)(Table S4) and remained significant after correcting for multiple testing. Dynamin-3 protein levels in striatum stratified by rs2421947 genotype (n=17) are not significantly higher for the GG genotype but there appears to be a trend (1.6 fold increase, p=0.08, Figure S6). We also observe significant differences in dynamin-3 localization in primary cortical neuronal cultures of *LRRK2* p.G2019S knock-in mice compared to wild-type (intensity and cluster density p<0.05; Figure S7).

Replication series

The *DNM3* association with AOO was examined in additional *LRRK2* p.G2019S carriers including subjects originating from Algeria (n=46), France (n=65), Norway (n=64) and North America (n=88). *DNM3* rs2421947 was imputed for the North American series using 1000

Genomes as a reference (described in Text S1), or was otherwise genotyped. Of note, the MAF for *LRRK2* carriers in each population series is different (Table S9). Cox proportional hazard ratios are provided for each population, censoring unaffected individuals, adjusting for family relatedness (Table S10) and gender as covariates, and combined within a meta-analysis that also adjusts for population in the model (HR 1.46 CI=1.04-2.04, p=0.02 for alternate homozygous genotypes) (Figure 3b).

Discussion

Unbiased genome-wide linkage analyses and locus-specific association, with replication of that association in an unrelated series, nominate *DNM3* as a genetic modifier of AOO in LRRK2 p.G2019S parkinsonism. The frequency of LRRK2 p.G2019S carriers is higher in North Africa than in any other region reported to date.^{2,3} Hence a strength of our study is the large number of patients and family members with LRRK2 p.G2019S originating from the same population. Clinical exams applied longitudinally by the same team of movement disorder specialists ensure accurate diagnoses and consistent data reporting. Inclusion of unrelated, incident cases at one site also avoids potential selection biases in referrals from multiple centers. The Arab-Berber population of Tunisia provides ethnic, genetic and environmental homogeneity to increase power for discovery. However, there are also many study limitations. In general, AOO is broadly defined and subjective: its variance is large even within *LRRK2* families although highly correlated with age of a motor diagnosis. Nevertheless, the variance in AOO in families is less than the variance in unrelated LRRK2 p.G2019S carriers suggestive of penetrance modifiers (Table 1a, median 56 years IQR=47-65 years). AOO is a fixed albeit temporal measure of disease pathophysiology. Hence, in our initial linkage and association analyses a dichotomized approach was used, using AOO about 56 years as a categorical variable. Key findings were assessed using Cox proportional hazards regression models censoring unaffected individuals, adjusting for family relatedness, gender and population series. It would be worthwhile to examine disease onset and progression in other ways. Longitudinal follow up of these families, additional patients and asymptomatic carriers is warranted.

Genome-wide linkage analysis to AOO was performed in large LRRK2 p.G2019S pedigrees employing informative STRs. The highest linkage peak identified is on chromosome

12 and is explained by LRRK2 p.G2019S. Families were selected based on this mutation and its “dominant” segregating haplotype. In Tunisia, several heterozygous ‘married in’ relatives and homozygous carriers are observed in highly consanguineous multi-incident pedigrees, and within the families 150 (59%) of carriers are affected (Table 1a). While the incidence of idiopathic PD is generally low (~2% at >65 years), and biologically carrier status and AOO may be independent, in our dataset this does not appear to be the case. Hence, we took a careful look at both the cis/trans effects of the *LRRK2* haplotype and association between AOO and common polymorphisms. Nevertheless, no significant effects were identified (data available on request). However, lack of evidence for association to AOO should not be considered evidence against. Our conclusion may reflect sample size, marker informativity or using AOO as the trait. Several case-control studies of idiopathic PD have highlighted association to LRRK2 coding³ and 5’ non-coding variability²². The second highest linkage peak is on chromosome 1q23.3-24.3 and remained robust when considering different models and allele frequencies. Significant association in the same locus was achieved with an independent series of unrelated LRRK2 p.G2019S carriers from the same population. Linkage peaks were present on chromosome 17q25.3 and 21q21.2 and LOD -1 interval 17q25.3 (75.2-77.0Mb) also showed significant evidence for association (rs4969113, p=0.0008). The signal is centromeric of the nearest gene, *LOC100134391*, that encodes a 296 amino acid protein of unknown function. Nevertheless, further investigation is warranted in larger datasets.

LRRK2 p.G2019S is a relatively rare, pathogenic mutation for disease. Thus our study was limited by the number of LRRK2 p.G2019S carriers available. In families, for linkage, the distribution of affected carriers was too sparse for AOO analysis as a continuous trait. However, as a dichotomized trait, we were able to include unaffected carriers’ age greater than or equal to

the median AAO. In addition, unaffected carriers younger than the median AAO were marked as ‘unknown’ status in pedigree analyses and thus contribute their genotype information. Hence, the significance of the *DNM3* finding may be driven by the inclusion of unaffected carriers older than the median AAO, not only affected carriers. Overall, in sporadic cases categorical (dichotomized) and quantitative approaches were informative; rs2421947 appears to have an effect on AAO of LRRK2 p.G2019S parkinsonism. Nevertheless, confidence intervals are wide and span 1.0 for several replication series, albeit relative to sample size, and the effect appears to be in the opposite direction for the French series. In addition, in the replication effort a major caveat is that convenience samples suffer an intrinsic ascertainment bias – as they are from patients with PD, of which a subset were found to be p.G2019S carriers.

Worldwide LRRK2 p.G2019S is generally inherited from the same ancestral haplotype² but the influence of modifiers and their associated allele frequencies may be population specific. There is suggestive linkage (LOD = 2.43) for AAO on chromosome 1q32.1 in predominantly North American LRRK2 p.G2019S families, albeit with no evidence for association in that genomic region in those samples.¹¹ Nevertheless, genome-wide association analysis of idiopathic PD in Japan robustly implicates PARK16 within 1q32,²² which is reproducibly observed albeit with low effect size (OR ~1.1) in a mega meta-analysis of Caucasian samples.²³ PARK16 includes *RAB29* (formerly *RAB7L1*) investigated as a candidate gene and associated with reduced risk of idiopathic and monogenic parkinsonism (LRRK2 p.G2019S and GBA p.N370S) in Ashkenazi.²⁴ Functional studies also support an interaction between RAB7L1, and LRRK2.^{25,26} Nevertheless, chromosome 1 linkage results in this and the previous study¹¹ appear independent. Patterns of linkage disequilibrium in Tunisian Arab-Berber and Israeli Jewish population samples are also different²⁷ thus additional tagging SNPs may be required to evaluate

DNM3 or other loci as penetrance modifiers. Gender has also been shown to influence AOO in *LRRK2* carriers with females having an earlier AOO compared to males, albeit controversial. In this study, gender does not influence the effect of *DNM3* rs2421947 in AOO.

Non-synonymous variability in *DNM3* was not observed in *LRRK2* carriers which allowed us to focus on polymorphic non-coding eQTLs (expression quantitative trait loci). Variability in *DNM3* expression correlates with genotype whether quantified by Ampliseq transcriptome or TaqMan methods. A specific isoform (Dyn3b) co-localizes with clathrin²⁸ and appears more highly expressed in *DNM3* rs2421947 GG homozygotes (Table S4, Figure S7). In striatum *DNM3* and *LRRK2* expression are correlated suggesting they are involved in the same process. *DNM3* rs2421947 does not appear to contribute to risk of idiopathic PD, neither susceptibility nor AOO, when comparing case-control in the Arab-Berber population (assessed by chi-square and regression analysis, data available on request), but the influence of *DNM3* rare variability has yet to be explored. Moreover, *DNM3* has not been nominated as a GWAS risk factor. Nonetheless, *DNM3* could be a specific modifier to *LRRK2* parkinsonism as the two interact biologically.

LRRK2 has been implicated in neurite outgrowth,^{29, 30} synaptic vesicle trafficking and neurotransmitter release, and via kinase-dependent mechanisms now directly shown to phosphorylate several Rab GTPase proteins.^{31 32} Much of the underlying mechanistic biology in these processes remains enigmatic, as does their clinical relevance to PD. However, our genetic study shows *DNM3* is an AOO modifier of *LRRK2* p.G2019S parkinsonism. *LRRK2* co-immunoprecipitates with the dynamin family GTPases that drive membrane fission (DNM1-3, and dynamin-related proteins)³³. Amphiphysin recruits dynamin and endophilin A (a *LRRK2* kinase substrate),³⁴ and recruits synaptojanin (SYNJ1) for endocytic vesicle fission.³⁵ Recessive

mutations in *SYNJ1* have been implicated in seizure disorders and early-onset parkinsonism.^{36, 37}

In neurons, dynamin-3 localizes to the endocytic machinery of dendritic spines to modulate receptor recycling and excitatory synaptic transmission.³⁸ In this process ‘Dyn3b’ isoform expression is also centrally involved in the regulation of actin polymerization, filopodia, and spine formation.^{28, 38} Intriguingly, a significant reduction and redistribution of dendritic dynamin-3 staining is observed in LRRK2 p.G2019S murine cortical cultures (Figure S7), although it may also reflect elevated glutamateric synaptic transmission.⁹

We postulated LRRK2 p.G2019S activates kinase activity,² an outcome of which has been the pursuit of competitive LRRK2 inhibitors. Based on similarly unbiased genetic data, we postulate lower levels of *DNM3*, and perhaps specific dynamin-3 isoforms, will delay the onset of LRRK2 p.G2019S parkinsonism. The crystal structure of the dynamin tetramer has just been elucidated,³⁹ and might accelerate the development of dynamin GTPase inhibitors (dynasores). These anticonvulsants repress synaptic transmission in seizure disorder⁴⁰ and delay alpha-synuclein uptake by neuronal and oligodendroglial cells.⁴¹ At autopsy, most LRRK2 p.G2019S carriers have alpha-synucleinopathy and Lewy body disease.^{42, 43} *DNM3* expression represents a target for neuroprotection in LRRK2 p.G2019S carriers, and potentially for disease-modification in *LRRK2* parkinsonism. Clinically, *DNM3* has been identified as a genetic modifier in this study of LRRK2 p.G2019S patients suggesting that this polymorphism should be a consideration in genetic counseling and future clinical trials.

Research in context

Evidence before this study

LRRK2 p.G2019S accounts for up to 40% of sporadic Parkinson's disease (PD) in Tunisia, 13-30% in Ashkenazi Jewish populations, and 1-2% in Caucasian populations. Carriers of *LRRK2* p.G2019S present a variable clinical phenotype, including incomplete penetrance, and a variable age at onset. This lead us to hypothesize that there are genetic factors that can modulate the phenoconversion of *LRRK2* p.G2019S, putatively by modulating the expression of other genes. Identification of these factors will provide a detailed understanding of molecular etiology and pathogenesis of disease. We searched PubMed for articles up to Nov 1, 2015, containing possible combinations of the terms "Parkinson's disease", "*LRRK2*", "genetic modifier", "disease modifiers" and "age at onset". We found two studies from 2012 suggesting a possible interaction of common variants in *SNCA* and *MAPT* that modifies age at onset in *LRRK2* p.G2019S carriers. We have previously tried to replicate the finding without success.

Added value of this study

LRRK2 influences synaptic transmission, immunity, endosomal trafficking, autophagy and mitochondrial metabolism, but the relevance of these pathways to the clinical pathophysiology of *LRRK2* p.G2019S parkinsonism remains unclear. Through linkage and haplotype association analysis we have identified a tagging SNP (rs2421947) in *DNM3*, for which the alternative allele reduces the age at onset of *LRRK2* p.G2019S carriers from Tunisia and in replication series. *DNM3* expression varies as a function of rs2421947 genotype in human striatum, and protein localization is perturbed in murine *LRRK2* p.G2019S knock-in cortical neurons.

Implications of all the available evidence

The discovery and replication of *DNM3* as a modifier of age at onset provides unbiased direction for *LRRK2* molecular neuroscience and future therapeutic development. *DNM3* expression represents a target for neuroprotection in *LRRK2* p.G2019S carriers and potentially for disease-

modification in LRRK2 p.G2019S parkinsonism. LRRK2 kinase inhibitors and dynamin GTPase inhibitors (dynasores) are already in pre-clinical development by several major Pharmaceutical firms. This discovery will have utility in genetic counselling, biomarker discovery and clinical trials.

Acknowledgements

The Canada Excellence Research Chairs (CERC), Leading Edge Endowment Fund (LEEF), National Institute on Aging, National Institute of Neurological Disorders and Stroke, the Michael J Fox Foundation, Mayo Foundation, Don Rix BC Leadership Chair in Genetic Medicine, the Roger de Spoelberch Foundation ,and GlaxoSmithKline has provided funding on patient recruitment, collection of data, generation of data and fellowships for researchers.

The authors wish to thank the many patients and their families who volunteered, and the longitudinal efforts of the many clinical teams involved. Initial studies in Tunisia on familial parkinsonism were in collaboration with Lefkos Middleton, Rachel Gibson, and the GlaxoSmithKline PD Programme Team (2002-2005). Subsequent clinical and molecular genetic analysis was supported through Mayo Foundation, GlaxoSmithKline, and National Institutes of Health (NINDS P50 NS40256; NINDS R21 NS064885; 2005-2009). The Michael J Fox Foundation generously supported clinical studies of LRRK2 p.G2019S in Tunisia, and subsequent whole genome sequencing (2008-2011). Molecular, bioinformatics and statistical analysis were funded through the Canada Excellence Research Chairs program (MF), CIHR/IRSC 275675 (2010-2017), and the Don Rix BC Leadership Chair in Genetic Medicine (MF, JT).

Replication series were made possible through the support of the France-Parkinson Association, the Roger de Spoelberch Foundation (R12123DD), the French program “Investissements d’avenir” (ANR-10-IAIHU-06). We thank the Research Council of Norway, Reberg’s legacy, and the Norwegian Parkinson Foundation. We also thank the Parkinson’s Study Group (PSG) PROGENI Investigators, Coordinators, and Molecular Genetic Laboratories. We acknowledge the Oxford Brain Bank, supported by the Medical Research Council (MRC), Brains for Dementia Research (BDR) (Alzheimer Society and Alzheimer Research UK), Autistica UK and the NIHR Oxford Biomedical Research Centre. Lastly, we thank the anonymous reviewers who’s efforts help make significant improvements to our statistical approach.

Contributions

MJF and JT designed the study and wrote the manuscript. JT, EMG, SB, MM, SL and RA performed the genetic experiments. JT, JK, AM, HH, LP, performed molecular and cellular analyses. JT, CVG, EN, JL, TF, AM and MF performed statistical analyses and data interpretation. JA, AB, MT, TF, RM, LP, SBS, EH, FN, EF and FH were responsible for clinical recruitment, data acquisition and analyses. MJF and FH supervised the study. All authors contributed to critical revision of the manuscript.

Declaration of interests

FH receives limited sponsorship from H. Lundbeck A/S for studies related to LRRK2 p.G2019S. Mayo Foundation, JA and MF have received royalty payments from Athena Diagnostics for USA Patent 7,544,786 related to LRRK2 p. G2019S. In addition, Mayo Foundation and MF have received royalties from H. Lundbeck A/S related to the development of LRRK2 murine

models including LRRK2 p.G2019S. Other authors report no disclosures relevant to the manuscript.

Figure legends

Figure 1. Overview of discovery and replication

Figure 2. Chromosome 1 linkage peak **a.** (LOD score = 4.99). **b.** Region of association within the LOD -1 linkage interval: Plink SNPs (10^{-5}) and Beagle haplotype ($p=1.06 \times 10^{-7}$) associations

Figure 3. Age-associated cumulative incidence of LRRK2 p.G2019S carriers.

a. Tunisian Arab-Berbers cumulative incidence of PD stratified by DN3 rs2421947 in Kaplan Meier **b.** Meta-Analysis of all populations (Algerian, French, Norwegian, North American and Tunisian Arab Berber) stratified by rs2421947 genotype ($p=0.02$).

Table 1a. Demographics of discovery cohorts: Tunisian Arab Berber LRRK2 p.G2019S carriers

Table 1b. Demographics of LRRK2 p.G2019S carriers: replication series

References

1. Zimprich A, Biskup S, Leitner P, Lichtner P, Farrer M, Lincoln S, et al. Mutations in LRRK2 cause autosomal-dominant parkinsonism with pleomorphic pathology. *Neuron*. 2004; **44**(4): 601-7.
2. Kachergus J, Mata IF, Hulihan M, Taylor JP, Lincoln S, Aasly J, et al. Identification of a novel LRRK2 mutation linked to autosomal dominant parkinsonism: Evidence of a common founder across European populations. *American Journal of Human Genetics*. 2005; **76**(4): 672-80.
3. Ross OA, Soto-Ortolaza AI, Heckman MG, Aasly JO, Abahuni N, Annesi G, et al. Association of LRRK2 exonic variants with susceptibility to Parkinson's disease: a case-control study. *Lancet Neurology*. 2011; **10**(10): 898-908.
4. Troiano AR, Elbaz A, Lohmann E, Belarbi S, Vidailhet M, Bonnet AM, et al. Low disease risk in relatives of north african lrrk2 Parkinson disease patients. *Neurology*. 2010; **75**(12): 1118-9.
5. Healy DG, Falchi M, O'Sullivan SS, Bonifati V, Durr A, Bressman S, et al. Phenotype, genotype, and worldwide genetic penetrance of LRRK2-associated Parkinson's disease: a case-control study. *Lancet Neurol*. 2008; **7**(7): 583-90.
6. Hentati F, Trinh J, Thompson C, Nosova E, Farrer MJ, Aasly JO. LRRK2 parkinsonism in Tunisia and Norway: a comparative analysis of disease penetrance. *Neurology*. 2014; **83**(6): 568-9.
7. Lesage S, Durr A, Tazir M, Lohmann E, Leutenegger AL, Janin S, et al. LRRK2 G2019S as a cause of Parkinson's disease in North African Arabs. *N Engl J Med*. 2006; **354**(4): 422-3.

8. Trinh J, Amouri R, Duda JE, Morley JF, Read M, Donald A, et al. Comparative study of Parkinson's disease and leucine-rich repeat kinase 2 p.G2019S parkinsonism. *Neurobiol Aging*. 2014; **35**(5): 1125-31.
9. Beccano-Kelly DA, Kuhlmann N, Tatarnikov I, Volta M, Munsie LN, Chou P, et al. Synaptic function is modulated by LRRK2 and glutamate release is increased in cortical neurons of G2019S LRRK2 knock-in mice. *Front Cell Neurosci*. 2014; **8**: 301.
10. Orenstein SJ, Kuo SH, Tasset I, Arias E, Koga H, Fernandez-Carasa I, et al. Interplay of LRRK2 with chaperone-mediated autophagy. *Nature neuroscience*. 2013; **16**(4): 394-406.
11. Latourelle JC, Hendricks AE, Pankratz N, Wilk JB, Halter C, Nichols WC, et al. Genomewide linkage study of modifiers of LRRK2-related Parkinson's disease. *Movement disorders : official journal of the Movement Disorder Society*. 2011; **26**(11): 2039-44.
12. Abecasis GR, Cherny SS, Cookson WO, Cardon LR. Merlin--rapid analysis of dense genetic maps using sparse gene flow trees. *Nat Genet*. 2002; **30**(1): 97-101.
13. Trinh J, Gustavsson EK, Guella I, Vilarino-Guell C, Evans D, Encarnacion M, et al. The role of SNCA and MAPT in Parkinson disease and LRRK2 parkinsonism in the Tunisian Arab-Berber population. *European journal of neurology : the official journal of the European Federation of Neurological Societies*. 2014; **21**(11): e91-2.
14. Purcell S, Neale B, Todd-Brown K, Thomas L, Ferreira MA, Bender D, et al. PLINK: a tool set for whole-genome association and population-based linkage analyses. *Am J Hum Genet*. 2007; **81**(3): 559-75.
15. Price AL, Patterson NJ, Plenge RM, Weinblatt ME, Shadick NA, Reich D. Principal components analysis corrects for stratification in genome-wide association studies. *Nat Genet*. 2006; **38**(8): 904-9.

16. Howey R, Cordell HJ. Imputation without doing imputation: a new method for the detection of non-genotyped causal variants. *Genet Epidemiol.* 2014; **38**(3): 173-90.
17. Browning BL, Browning SR. Haplotypic analysis of Wellcome Trust Case Control Consortium data. *Hum Genet.* 2008; **123**(3): 273-80.
18. Browning BL, Browning SR. A unified approach to genotype imputation and haplotype-phase inference for large data sets of trios and unrelated individuals. *Am J Hum Genet.* 2009; **84**(2): 210-23.
19. Hulihan MM, Ishihara-Paul L, Kachergus J, Warren L, Amouri R, Elango R, et al. LRRK2 Gly2019Ser penetrance in Arab-Berber patients from Tunisia: a case-control genetic study. *Lancet Neurol.* 2008; **7**(7): 591-4.
20. Ishihara-Paul L, Hulihan MM, Kachergus J, Upmanyu R, Warren L, Amouri R, et al. PINK1 mutations and parkinsonism. *Neurology.* 2008; **71**(12): 896-902.
21. Hauser ER, Watanabe RM, Duren WL, Bass MP, Langefeld CD, Boehnke M. Ordered subset analysis in genetic linkage mapping of complex traits. *Genet Epidemiol.* 2004; **27**(1): 53-63.
22. Satake W, Nakabayashi Y, Mizuta I, Hirota Y, Ito C, Kubo M, et al. Genome-wide association study identifies common variants at four loci as genetic risk factors for Parkinson's disease. *Nat Genet.* 2009; **41**(12): 1303-7.
23. Nalls MA, Pankratz N, Lill CM, Do CB, Hernandez DG, Saad M, et al. Large-scale meta-analysis of genome-wide association data identifies six new risk loci for Parkinson's disease. *Nat Genet.* 2014; **46**(9): 989-93.

24. Gan-Or Z, Bar-Shira A, Dahary D, Mirelman A, Kedmi M, Gurevich T, et al. Association of sequence alterations in the putative promoter of RAB7L1 with a reduced parkinson disease risk. *Arch Neurol*. 2012; **69**(1): 105-10.
25. MacLeod DA, Rhinn H, Kuwahara T, Zolin A, Di Paolo G, McCabe BD, et al. RAB7L1 interacts with LRRK2 to modify intraneuronal protein sorting and Parkinson's disease risk. *Neuron*. 2013; **77**(3): 425-39.
26. Beilina A, Rudenko IN, Kaganovich A, Civiero L, Chau H, Kalia SK, et al. Unbiased screen for interactors of leucine-rich repeat kinase 2 supports a common pathway for sporadic and familial Parkinson disease. *Proceedings of the National Academy of Sciences of the United States of America*. 2014; **111**(7): 2626-31.
27. Carmi S, Hui KY, Kochav E, Liu X, Xue J, Grady F, et al. Sequencing an Ashkenazi reference panel supports population-targeted personal genomics and illuminates Jewish and European origins. *Nature communications*. 2014; **5**: 4835.
28. Cao H, Garcia F, McNiven MA. Differential distribution of dynamin isoforms in mammalian cells. *Mol Biol Cell*. 1998; **9**(9): 2595-609.
29. MacLeod D, Dowman J, Hammond R, Leete T, Inoue K, Abeliovich A. The familial Parkinsonism gene LRRK2 regulates neurite process morphology. *Neuron*. 2006; **52**(4): 587-93.
30. Parisiadou L, Xie C, Cho HJ, Lin X, Gu XL, Long CX, et al. Phosphorylation of ezrin/radixin/moesin proteins by LRRK2 promotes the rearrangement of actin cytoskeleton in neuronal morphogenesis. *J Neurosci*. 2009; **29**(44): 13971-80.
31. Arranz AM, Delbroek L, Van Kolen K, Guimaraes MR, Mandemakers W, Daneels G, et al. LRRK2 functions in synaptic vesicle endocytosis through a kinase-dependent mechanism. *J Cell Sci*. 2015; **128**(3): 541-52.

32. Steger M, Tonelli F, Ito G, Davies P, Trost M, Vetter M, et al. Phosphoproteomics reveals that Parkinson's disease kinase LRRK2 regulates a subset of Rab GTPases. *Elife*. 2016; **5**.
33. Stafa K, Tsika E, Moser R, Musso A, Glauser L, Jones A, et al. Functional interaction of Parkinson's disease-associated LRRK2 with members of the dynamin GTPase superfamily. *Hum Mol Genet*. 2014; **23**(8): 2055-77.
34. Matta S, Van Kolen K, da Cunha R, van den Bogaart G, Mandemakers W, Miskiewicz K, et al. LRRK2 controls an EndoA phosphorylation cycle in synaptic endocytosis. *Neuron*. 2012; **75**(6): 1008-21.
35. Ferguson SM, De Camilli P. Dynamin, a membrane-remodelling GTPase. *Nature reviews Molecular cell biology*. 2012; **13**(2): 75-88.
36. Krebs CE, Karkheiran S, Powell JC, Cao M, Makarov V, Darvish H, et al. The Sac1 domain of SYNJ1 identified mutated in a family with early-onset progressive Parkinsonism with generalized seizures. *Hum Mutat*. 2013; **34**(9): 1200-7.
37. Quadri M, Fang M, Picillo M, Olgiati S, Breedveld GJ, Graafland J, et al. Mutation in the SYNJ1 gene associated with autosomal recessive, early-onset Parkinsonism. *Hum Mutat*. 2013; **34**(9): 1208-15.
38. Gray NW, Kruchten AE, Chen J, McNiven MA. A dynamin-3 spliced variant modulates the actin/cortactin-dependent morphogenesis of dendritic spines. *J Cell Sci*. 2005; **118**(Pt 6): 1279-90.
39. Reubold TF, Faelber K, Plattner N, Posor Y, Ketel K, Curth U, et al. Crystal structure of the dynamin tetramer. *Nature*. 2015.

40. Li YY, Chen XN, Fan XX, Zhang YJ, Gu J, Fu XW, et al. Upregulated dynamin 1 in an acute seizure model and in epileptic patients. *Synapse*. 2015; **69**(2): 67-77.
41. Konno M, Hasegawa T, Baba T, Miura E, Sugeno N, Kikuchi A, et al. Suppression of dynamin GTPase decreases alpha-synuclein uptake by neuronal and oligodendroglial cells: a potent therapeutic target for synucleinopathy. *Mol Neurodegener*. 2012; **7**: 38.
42. Ross OA, Toft M, Whittle AJ, Johnson JL, Papapetropoulos S, Mash DC, et al. Lrrk2 and Lewy body disease. *Annals of neurology*. 2006; **59**(2): 388-93.
43. Kalia LV, Lang AE, Hazrati LN, Fujioka S, Wszolek ZK, Dickson DW, et al. Clinical correlations with Lewy body pathology in LRRK2-related Parkinson disease. *JAMA Neurol*. 2015; **72**(1): 100-5.

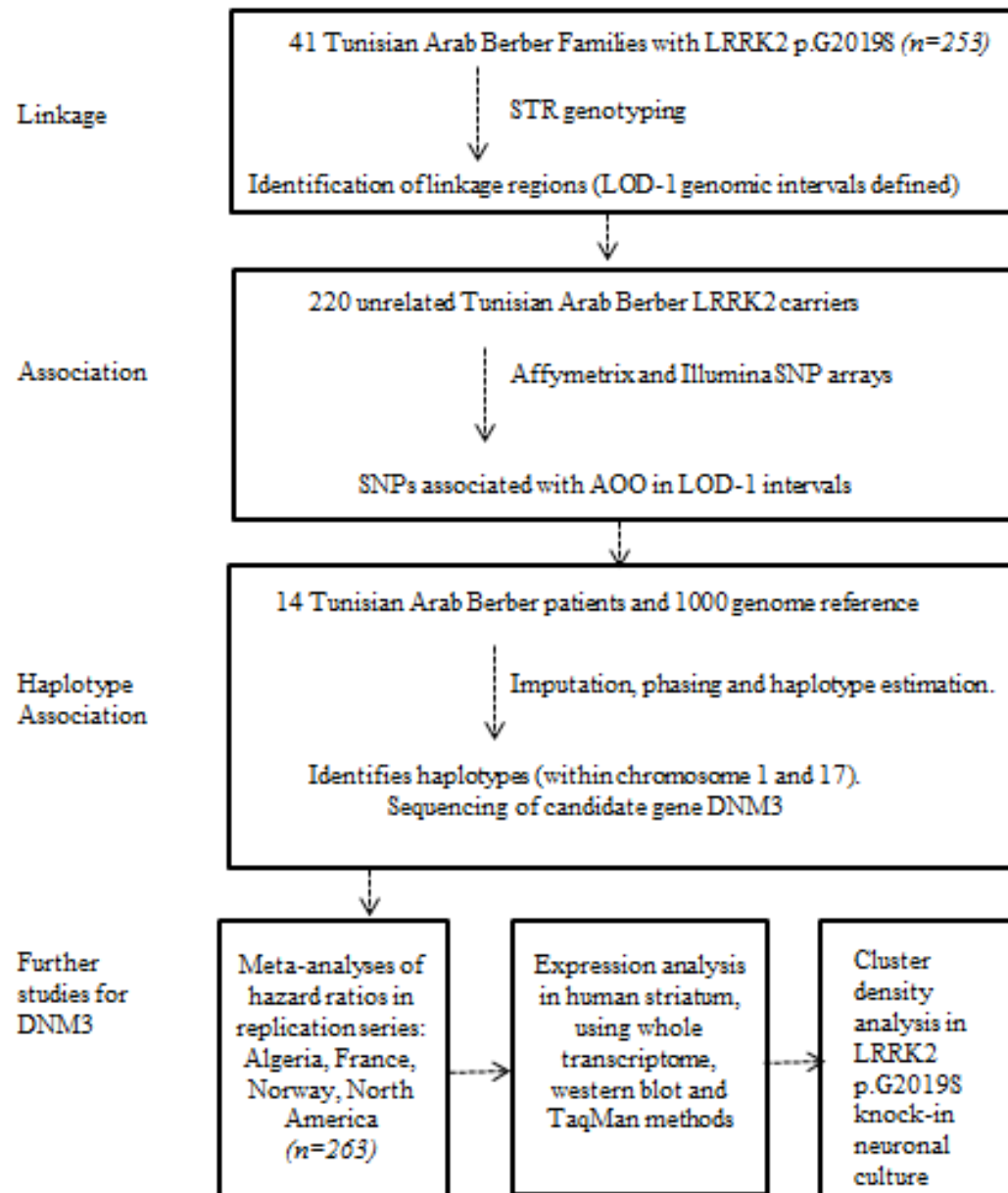


Figure 1. Overview of discovery and replication

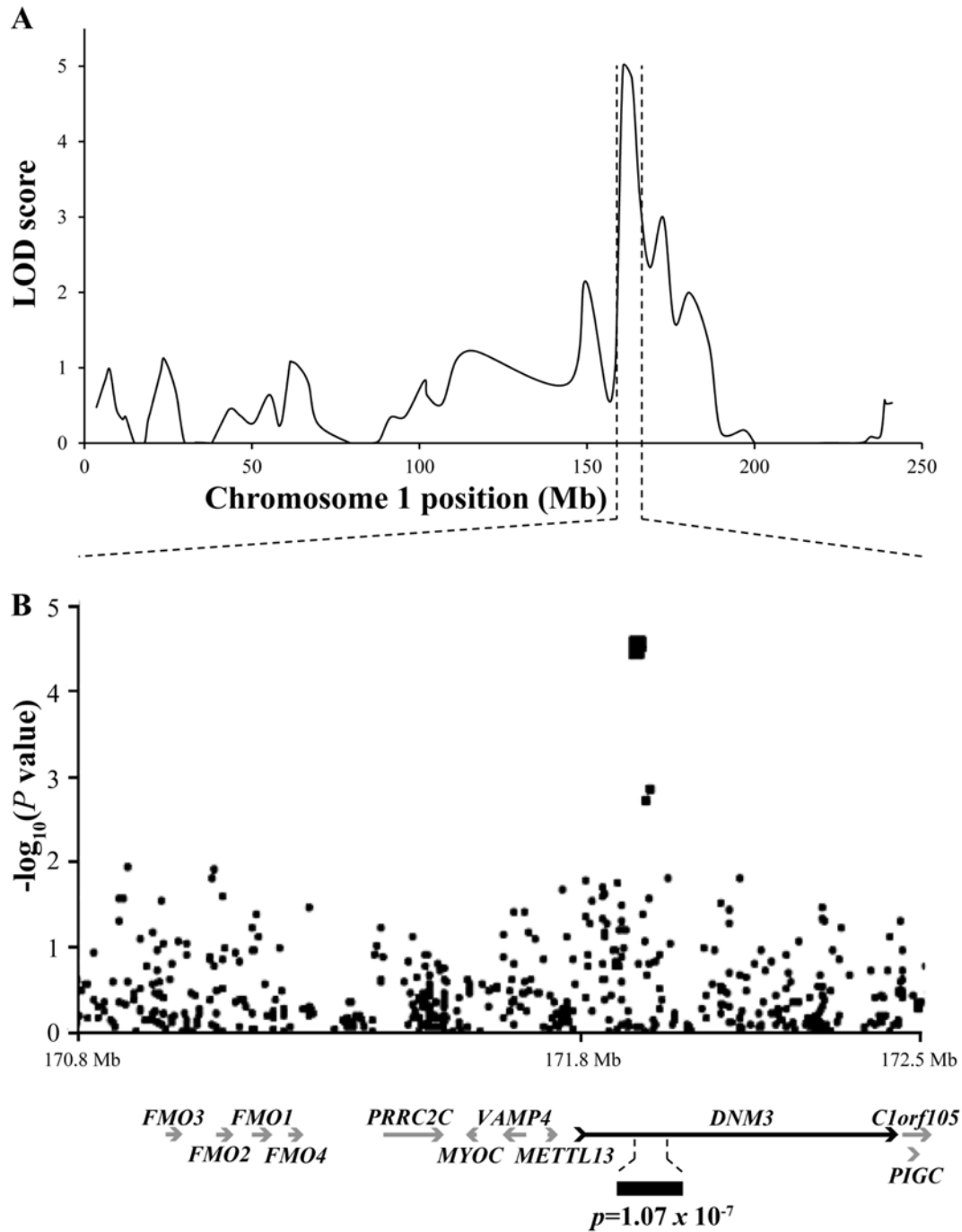


Figure 2. Chromosome 1 linkage peak

a. (LOD score = 4.99). **b.** Region of association within the LOD -1 linkage interval: Plink SNPs (10^{-5}) and Beagle haplotype ($p=1.06 \times 10^{-7}$) associations

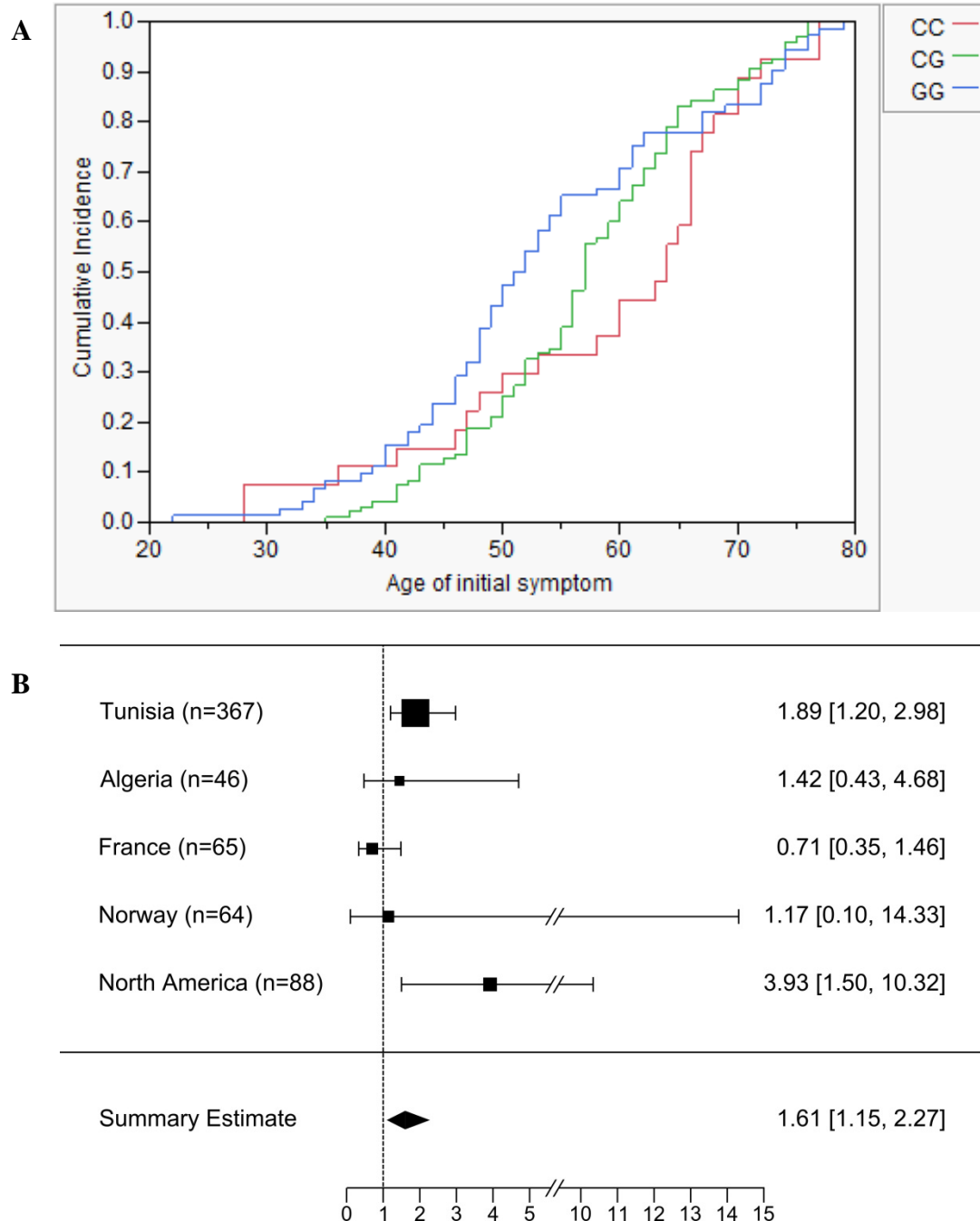


Figure 3. Age-associated cumulative incidence of LRRK2 p.G2019S carriers.

a. Tunisian Arab-Berbers cumulative incidence of PD stratified by DNM3 rs2421947 in Kaplan Meier **b.** Meta-Analysis of all populations (Algerian, French, Norwegian, North American and Tunisian Arab Berber) stratified by rs2421947 genotype ($p=0.02$).

Table 1a. Demographics of discovery cohorts: Tunisian Arab Berber LRRK2 p.G2019S carriers

	Sporadic patients with PD	Unrelated control subjects	Familial Parkinsonism	Unaffected family members
N	220	12	150	103
Number of men (%)	124 (56%)	6 (50%)	77 (51.3%)	48 (46.6%)
Mean age (SD) years	67.6 (12.6)	56.7 (10.9)	68.6 (15.8)	56.1 (17.5)
Median age (IQR)	69 (48-90)	54.5 (38-72)	70.5 (57-81)	53 (43-72.5)
Mean age of onset (SD)	57.1 (11.6)	-	56.1 (12.8)	-
Median age of onset (IQR)	57 (40-74)	-	56 (47-65)	-

* The unrelated patient series are largely clinic-based convenience samples

Table 1b. Demographics of LRRK2 p.G2019S carriers: replication series

	Algeria		France		Norway		North America		Total
	Patient	Unaffected	Patient	Unaffected	Patient	Unaffected	Patient	Unaffected	
N	45	1	48	17	19	45	88	-	263
Number of men (%)	19 (42%)	-	26 (60%)	7 (39%)	8 (42%)	18 (40%)	41(47%)	-	
Mean age (SD) years	55.5 (11.3)	54	57.7 (13.8)	67.4 (11.8)	67.6 (17.5)	63.6 (12.4)	NA	-	
Median age (IQR)	55 (45.3-63)	54	59 (46.8-67.3)	67 (59.5-76.8)	73 (52-82)	62 (54.5-70)	NA	-	
Mean age of onset (SD)	49.6 (10.3)	-	52.1 (13.5)	-	62.6 (13.0)	-	61.5 (10.1)	-	
Median age of onset (IQR)	50 (43-56)	-	51 (41.3-62)	-	65 (49-74)	-	63 (56-70)	-	

* The replication series are largely based on convenience samples. There are 145 unrelated subjects and 118 related subjects.

Supplementary Appendix

This appendix has been provided by the authors to give readers additional information about their work.

Table of contents	Content	Page number
Text S1	Descriptive statistics for beagle imputation, haplotype association, expression analysis	3
Table S1.	Demographics of healthy control brains for expression analysis	4
Table S2.	Primer pairs and custom TaqMan probe design for different dynamin-3 transcript isoforms	5
Table S3.	<ul style="list-style-type: none"> a. PLINK association underneath linkage region b. Age at onset quantitative analysis with Cox proportional hazard model c. <i>DNM3</i> Beagle haplotypes associated with AAO as dichotomized trait d. <i>DNM3</i> Beagle haplotypes associated with AAO as continuous trait 	6-8
Table S4.	<i>DNM3</i> levels of highly correlate with <i>LRRK2</i> , <i>VPS35</i> , <i>SYNJ1</i> in stratum tissue transcriptome data of healthy control subjects (n=17)	9
Table S5.	Sensitivity analysis for different cut-offs on chromosome 1q23.3-24.3 using non-parametric linkage	9
Table S6-9	<i>DNM3</i> SNP rs2421947 minor allele frequencies	10
Table S10	Family Relatedness in Cox-proportional Hazards model	11
Figure S1.	Whole genome sequencing and Imputation workflow	12
Figure S2.	A schematic of the Dynamin isoforms; primers are represented with arrows. Figure adapted from Cao et al 1998	13
Figure S3.	Multipoint model-based and nonparametric linkage analysis of Tunisian Arab-Berber <i>LRRK2</i> p.G2019S families	14 and 15
Figure S4.	Chromosome 1 Q-Q plot values	16
Figure S5.	<i>DNM3</i> transcript levels	17
Figure S6.	Dynamin-3 protein levels	18
Figure S7.	Dynamin-3 staining in cortical neurons A. representative confocal microscopic images of dynamin-3 (red), MAP2 (blue) in wild-type (WT) and GKI (heterozygous <i>LRRK2</i> p.G2019S knock- in) murine cortical neurons.	19
	Supplementary references	20

Text S1. Descriptive statistics for linkage, association and expression analysis

Linkage was performed with Merlin¹. Age of onset was stratified <56 or ≥56 years (AOO dichotomized model) and as a quantitative (continuous) trait. For the former, phenotypic coding in the pedigree file has 0=missing information or non-carriers of LRRK2 p.G2019S, 1=AOO <56 LRRK2 p.G2019S, 2=AOO ≥56 LRRK2 p.G2019S. Sensitivity analysis using different AOO cut-offs was performed (Table S5). Loci with suggestive linkage (NPL>2.0 & model-based LOD>3.3), which remained robust to different AOO cut-offs, were nominated. Within those linked regions maximum LOD-1 genomic intervals were defined.

SNPs within each LOD -1 region were extracted and managed using PLINK, merging Affymetrix and MEGA datasets. SNP quality control was performed (>95% genotype call rate and >95% of marker). Genome-wide IBS/IBD (identity by state/identity by descent) estimates were used to identify and exclude sample contamination, duplicates and seemingly related individuals. Population stratification was assessed with Eigenstrat². Association analyses for AOO were performed with Cox proportional hazard models. The dataset included the original families and a separate Arab Berber dataset of unrelated, affected LRRK2 p.G2019S carriers. Analyses adjusted for family relatedness and gender.

For LOD -1 regions, with evidence of both linkage and association, PLINK SNP files were converted into VCF files with PLINK/SEQ. Beagle 4.0 was used for loci imputation, employing whole genome sequences of Tunisian Arab Berber subjects (n=14) and 1000 Genomes data. Burn-in, phase and imputation iterations were set at 10 to maximize genotype imputation accuracy. Beagle 3.3 was subsequently used to estimate and define haplotypes (as diallelic pseudomarkers). Haplotype association analyses were performed with an Arab Berber dataset of unrelated, affected LRRK2 p.G2019S carriers using AOO as a dichotomized or quantitative trait. Linear regression was adjusted for gender and corrected p-values for haplotype association and multiple-testing were estimated by permutation analyses, randomizing group membership. Dynamin 3 (*DNM3*) was the only candidate gene highlighted by association and was sequenced to identify coding variants. The *DNM3* assignment (rs2421947) with AOO was assessed in clinic-based samples from four additional populations including a meta-analysis of hazards ratios.

Analysis of *DNM3* expression was conducted. Total RNA was extracted (RNeasy Qiagen Minikit) in duplicate samples from human striatum (n=61 control subjects) and DNase I digested prior to assessing the concentration, quality and RNA integrity (RIN) with an Agilent 2100 bioanalyzer, RNA 6000 LabChip kit and associated software (Agilent). Thirty-eight control striatum had a RIN >7.0 and were used for TaqMan analysis. *DNM3* transcripts were measured using Taqman probe IDs Hs00399015_m1 (all transcripts) and Hs00927940_m1 (NM_001136127.2 and NM_015569.4 only). Three commonly used “housekeeping” genes: hypoxanthine phosphoribosyl-transferase (*HPRT*; Hs02800695_m1), glyceraldehyde-3-phosphate dehydrogenase (*GAPDH*; Hs02758991_g1) and synaptophysin (*SYP*; Hs00300531_m1) were measured as a control. *DNM3* transcript levels were normalized by dividing 2-Ct by the geometric mean of control gene expression, adjusted by RIN quality. The subset of samples homozygous for alternate *DNM3* rs2421947 genotypes was also evaluated using AmpliseqTM whole human transcriptome analysis (n=17), performed with an Ion Proton (Life Technologies, Inc). In brief, high-quality, total RNA was reverse-transcribed and amplified using TaqMan One Step RT-PCR kit following manufacture’s protocol (ABI). Sequencing analysis resulted in an average of over 12 million reads per sample and a read length of 114 bases. AmpliseqRNA was used to map reads and generate absolute/normalized gene expression values (reads per million, RPM). Ampliseq Transcriptome data was normalized with a variety of housekeeping genes (*GAPDH*, *HPRT*, *SYP*, *YWHAZ*) including those primarily expressed in neurons (*TH*, *MAP2*, *ENO2*, *SV2A*, *SV2B*, *SYN1*, *SYN2*) and the expression findings were robust. Spearman’s correlation coefficient is reported between rs2421947 and *DNM3* expression, under an additive model. Further analysis was done by regression, correcting for gender and RIN. For protein analysis, 20mg brain tissue (n=17) was lysed with buffer containing 1% NP-40, 20mM HEPES, 125mM NaCl, 50mM NaF and protease inhibitor cocktail (Roche). Lysates were put on ice for 1 hour. Blotting of dynamin-3 was done with a polyclonal rabbit antibody (Synaptic Systems [115 302], 1:1000) and with a mouse monoclonal antibody for GAPDH (Thermo Scientific [MA5-15738], 1:1000). Dynamin-3 and MAP2 antibodies (Abcam) were used in immunofluorescence (1:1000) of primary neuronal LRRK2 p.G2019S knock-in cultures, as previous.⁴

Table S1. Demographics of healthy control subjects and brains for expression analysis

Control subjects	
N	61
Number of men (%)	30 (49.2%)
Mean age at death (SD) years	80.6 (12.1)
Median age at death (IQR)	85 (71-89)
Tissue type	Striatal
Average RIN (RNA integrity number) (SD)	8.6 (1.2)
Average PMI (Post-mortem interval) (SD)	48.8 (33.2)

Table S2. Primer pairs and custom TaqMan probe design for *DNM3* transcripts in human striatum

Names	5'→3' Primers	Amino acid sequence
Region 1		
DNM3_Reg1F	<u>aaacggaaaggattgttc</u>	
DNM3_Reg1Fprobe	<u>tctctacatcaacaccaacc</u>	
DNM3_Reg1BR	<u>ccctgcgaatcacaatttg</u>	GTNLPPSRQI
DNM3_Reg1AR	ttgcgaatcacctgatttc	//
DNM3_Reg1C_F	gcaaattgtacgagctaagttc	VRAKFCKLYCCFFI
DNM3_Reg1_R	ttcaggtgtccaagggaag	
Region 2		
DNM3_Reg2A_F	<u>tatcctgacaaatctgtagctg</u>	SVAEN
DNM3_Reg2_R	ggctcctctgaagaatacaac	
DNM3_Reg2B_F	tctgtagggaacaacaaagc	SVGNNKAEN
DNM3_Reg2_R	ggctcctctgaagaatacaac	
Region 3		
DNM3_Reg3_F	aaaggaggccaacactaag	SRRPPSPTRPTIIRP...
DNM3_Reg3B_R	attatagtgggacgagttgg	
DNM3_Reg3_F	aaaggaggccaacactaag	RFGAMKDEAAEP
DNM3_Reg3A_R	cagcagcttcacctcatgg	
Probe		
TaqMan Probe design	attggcttcgcaaatgctcagcagag	

Table S3a. PLINK association within regions of linkage (LOD-1 support intervals)

CHR	SNP	BP	A1	F_A	F_U	A2	CHISQ	P	OR
1	rs742510	171858930	A	0.5	0.1974	G	18.13	2.06 x 10 ^{-5**}	4.067
1	rs2421947	171833094	C	0.5	0.1974	G	18.13	2.06 x 10 ^{-5**}	4.067
1	rs2206543	171835493	G	0.5	0.1974	A	18.13	2.06 x 10 ^{-5**}	4.067

** Values significant after Bonferroni correction for all SNP association tests within the LOD-1 linkage interval on chr 1

Table S3b. Quantitative analysis of AOO (Cox proportional hazard modelling)

SNP	Chr	Position	Nearby Gene	HR	HR lower 95%	HR upper 95%	p-value
rs2421947	1	171833094	<i>DNM3</i>	1.89	1.20	2.98	0.0053

Estimates are adjusted for gender and familial relationship, unaffected carriers are censored

SNP	Chr	Position	Nearby Gene	HR	HR lower 95%	HR upper 95%	p-value
rs4969113	17	68873429	<i>SDK2/LOC100134391</i>	3.35	1.65	6.82	0.0008

Estimates are adjusted for gender and familial relationship, unaffected carriers are censored

SNP	Chr	Position	Nearby Gene	HR	HR lower 95%	HR upper 95%	p-value
rs986917	21	22869596	<i>NCAM2</i>	0.38	0.20	0.72	0.0027
rs382816	21	20296035		2.51	1.37	4.59	0.0028

Estimates are adjusted for gender and familial relationship, unaffected carriers are censored

Table S3c. *DNM3* haplotypes associated with AAO (as a dichotomized trait)

rs77565020	rs75848807	rs192895361	rs74673993	rs142760983	rs559149705	rs185844670	rs541736672	rs563254497	rs530428455	rs190417579	rs74777828	rs192302781	rs146042960	rs566301333	rs376575981	rs183688167	rs114979811	rs56237038	rs72713714	rs2421947	count	p-value
Major haplotypes:																						
G	G	G	T	A	G	G	A	A	C	A	T	A	T	G	A	G	T	A	G	G	238	1.07E-07**
G	G	G	T	A	G	G	A	A	C	A	T	A	T	G	A	G	T	A	G	C	138	0.122
Minor haplotypes:																						
G	A	G	T	A	G	G	A	A	C	A	T	A	T	G	A	G	T	A	G	C	1	NA
G	G	G	T	A	G	G	A	A	C	A	A	A	T	G	A	G	T	A	G	C	5	NA
G	G	G	T	A	G	G	A	A	C	A	T	A	T	G	A	G	T	A	C	C	3	NA
G	A	G	T	A	G	G	A	A	C	A	T	A	T	G	A	G	T	A	C	C	1	NA
G	A	G	T	A	G	G	A	A	C	A	T	A	T	G	A	G	T	A	G	G	2	0.515
G	G	G	T	A	G	G	A	A	C	A	T	A	T	G	A	G	T	A	C	G	1	0.411

** Values significant after permutation for all haplotype associations within the LOD -1 linkage interval on chr 1

Table S3d. Haplotypes associated with AAO (as a quantitative trait)

***DNM3* haplotype**

rs77565020	rs75848807	rs192895361	rs74673993	rs142760983	rs559149705	rs185844670	rs541736672	rs563254497	rs530428455	rs190417579	rs74777828	rs192302781	rs146042960	rs566301333	rs376575981	rs183688167	rs114979811	rs56237038	rs72713714	rs2421947	p-value
Major haplotypes:																					
G	G	G	T	A	G	G	A	A	C	A	T	A	T	G	A	G	T	A	G	G	0.00028**

** Values significant after permutation for all haplotype associations within the LOD -1 linkage interval on chr 1

Nearest gene: *LOC100134391*

rs2683172	rs17836849	rs7208077	rs16977764	rs9909402	rs9907041	rs2353109	p-value
Major haplotypes:							
T	G	T	A	T	A	C	0.00071**

** Values significant after permutation for all haplotype associations within the LOD -1 linkage interval on chr 17

Table S4. *DNM3* transcript levels correlate with *LRRK2*, *VPS35* and *SYNJ1* expression in striatal tissue transcriptome data from normal controls (n=17).

Gene	<i>DNM3</i> expression level correlation coefficient	p-value
<i>Late-onset autosomal dominant</i>		
<i>LRRK2</i>	0.65	0.004**
<i>VPS35</i>	0.65	0.008
<i>SNCA</i>	0.65	0.04
<i>DNAJC13</i>	0.21	0.14
<i>Early-onset recessive</i>		
<i>SYNJ1</i>	0.41	0.008
<i>PINK1</i>	0.53	0.02
<i>PARK2</i>	0.21	0.04
<i>FBXO7</i>	0.51	0.12

**Values significant after Bonferroni correction

Table S5. Sensitivity analysis for linkage using a dichotomized model with different AAO cut-offs

Age at onset dichotomization	Chromosome 1q23.3-24.3 NPL LOD score
45 years	2.3
50 years	2.5
55 years	2.9
60 years	1.8
65 years	1.2

Table S6-9. *DNM3* SNP rs2421947 minor allele frequencies

<i>DNM3</i> rs2421947 in control subjects*	Age
MAF C=0.39 (n=74)	≥70
MAF C=0.42 (n=162)	≥60
MAF C=0.43 (n=265)	≥50
MAF C=0.43 (n=313)	≥40
MAF C=0.43 (n=317)	≥30

* Tunisian Arab-Berber population series. Age is calculated based on year of birth.

Affected <i>LRRK2</i> carriers	Age at onset
MAF C=0.44 (n=31)	≥70
MAF C=0.50 (n= 86)	≥60
MAF C=0.46 (n=147)	≥50
MAF C=0.39 (n=191)	≥40
MAF C=0.39 (n=208)	≥30

* Tunisian Arab-Berber population series.

All <i>LRRK2</i> carriers	Age
MAF C=0.43 (n=90)	≥70
MAF C=0.38 (n=131)	≥60
MAF C=0.36 (n=187)	≥50
MAF C=0.39 (n=201)	≥40
MAF C=0.39 (n=220)	≥30

* Tunisian Arab-Berber population series. Excludes unaffected *LRRK2* p.G2019S carriers. Age is calculated based on year of birth.

Population series	MAF
Tunisian	0.39
Algerian	0.39
French	0.41
Norway	0.70
America	0.52

*Only unrelated probands and sporadic patients with *LRRK2* p.G2019S included

Table S10. Replication series detailed demographics

	Unrelated sporadic patients	Unrelated probands	Number of families	Number of family members (kinship coefficient)	Total (n)
Tunisia	232	41	41	49 (0.5)	367
				23 (0.25)	
				22 (0.125)	
Algeria	43	1	1	2 (0.5)	46
France	39	5	5	9 (0.5)	65
				3 (0.25)	
				9 (0.125)	
Norway	2	12	12	22 (0.5)	64
				11 (0.25)	
				17 (0.125)	
North America	0	43	43	45 (0.5)	88

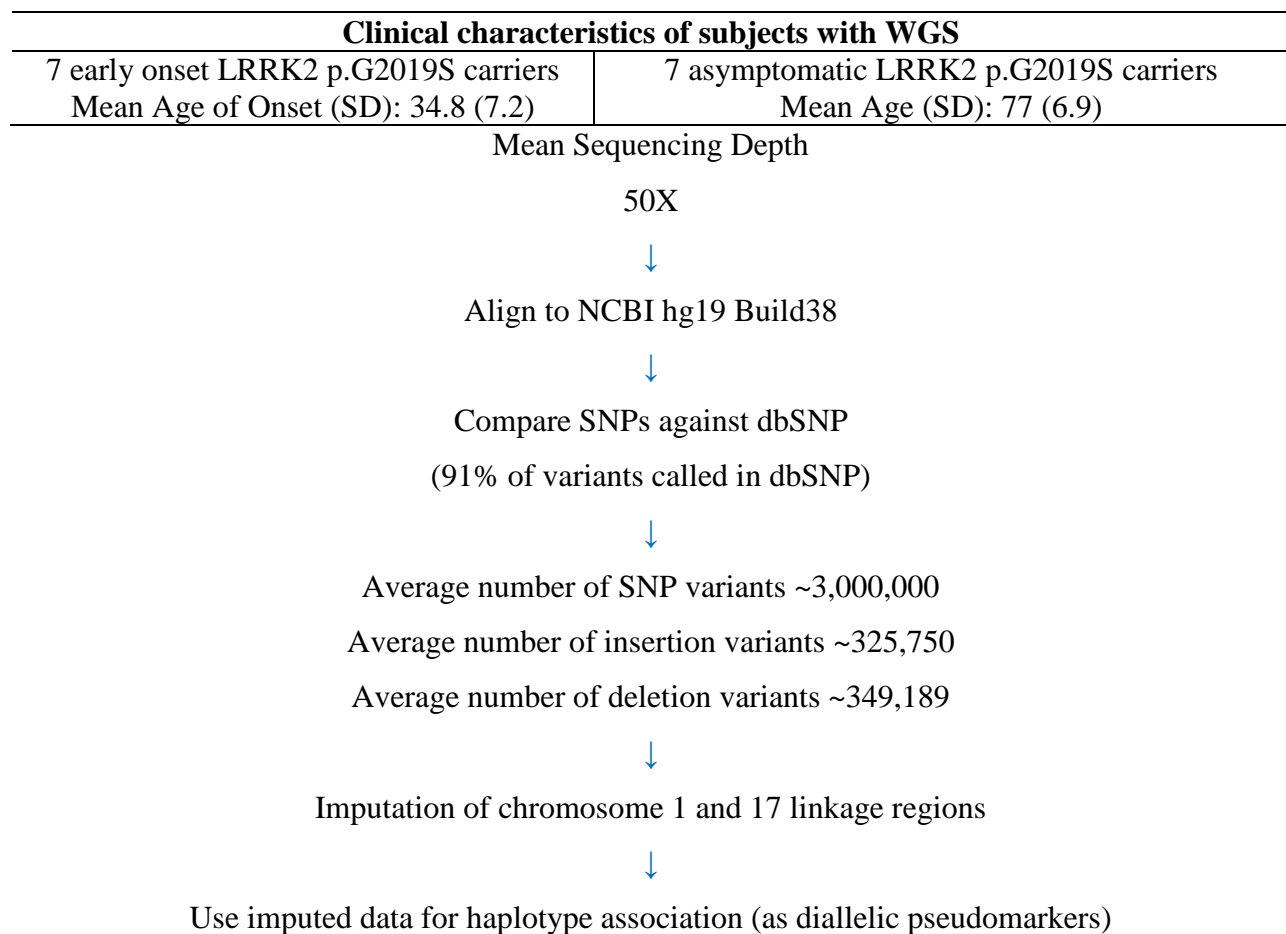


Figure S1. Whole genome sequencing and imputation workflow

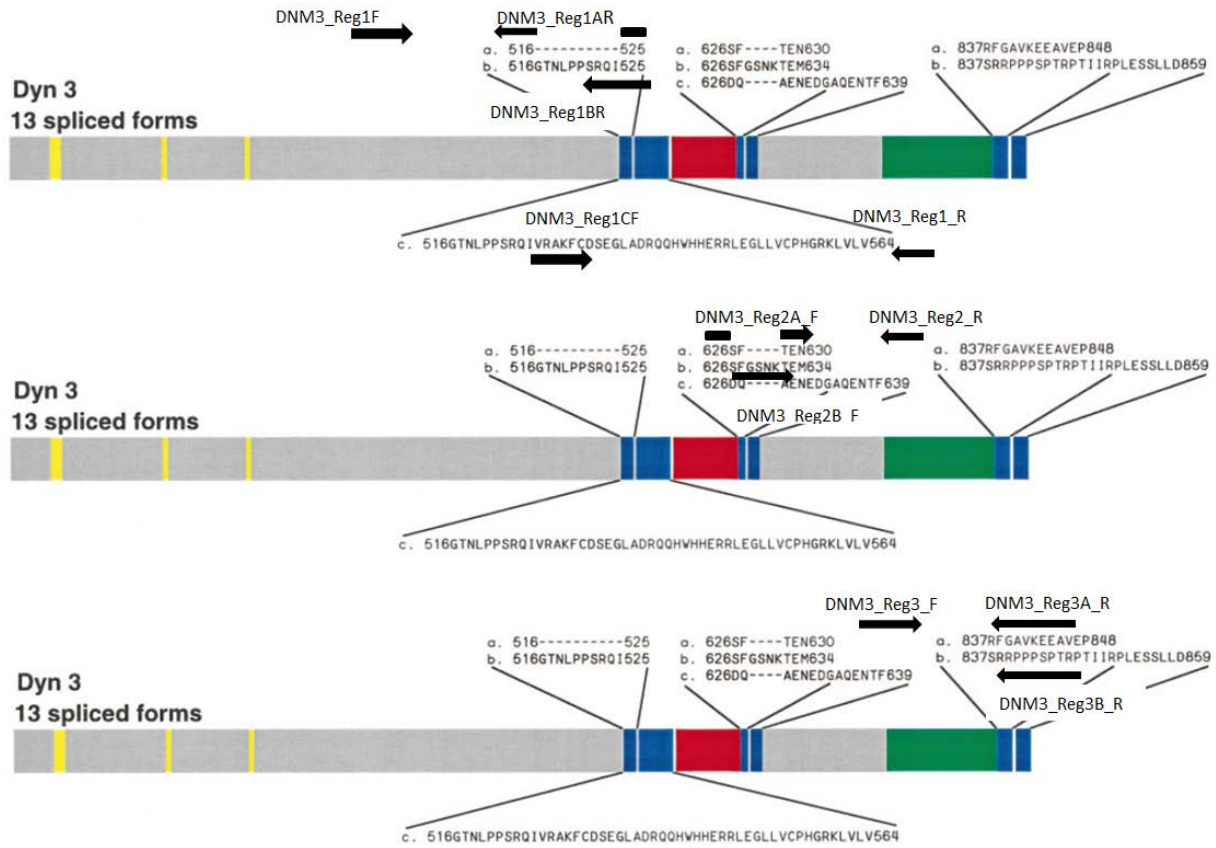
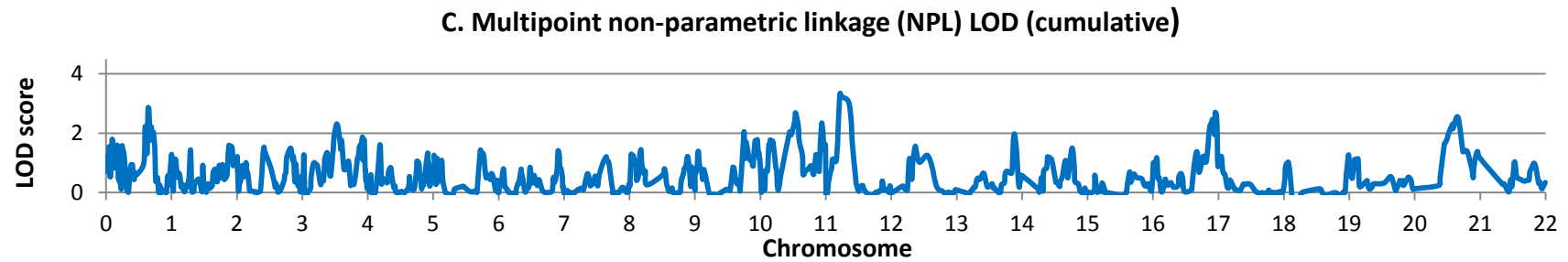
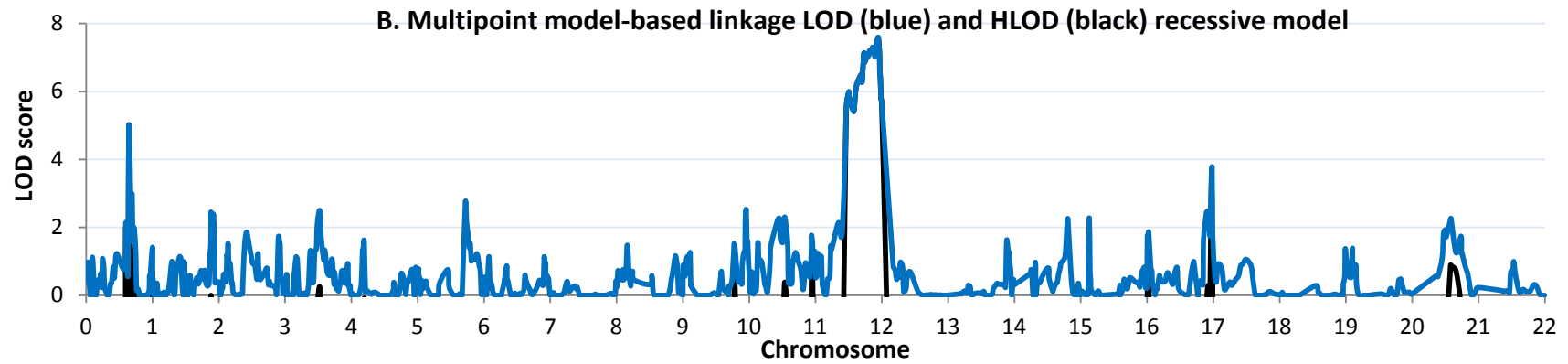
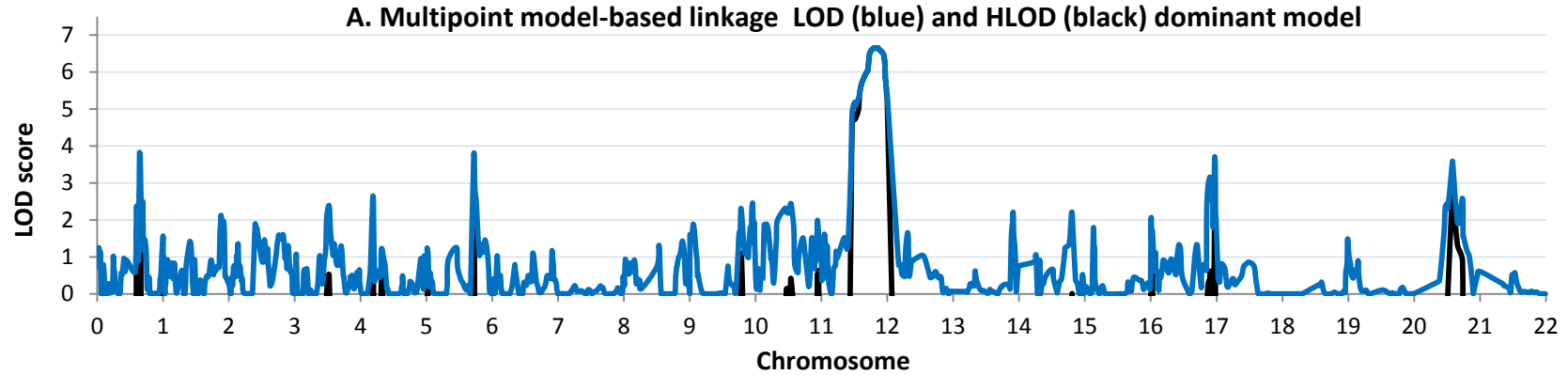


Figure S2. A schematic of the thirteen dynamin isoforms; primers are represented with arrows. Figure adapted from Cao et al³.



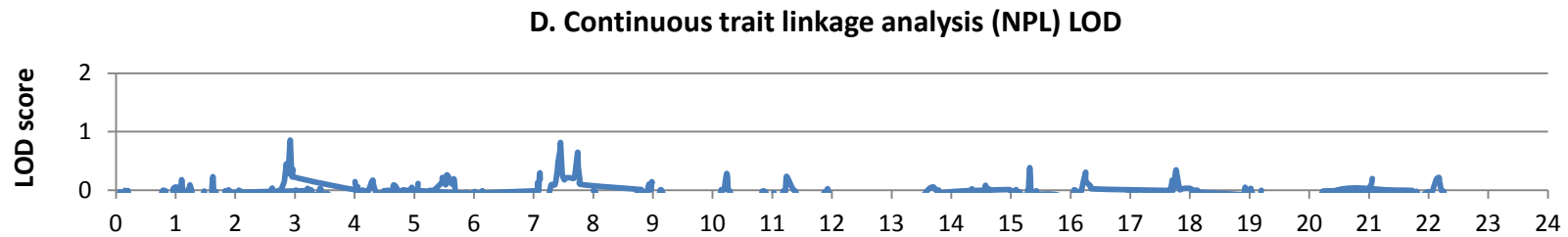


Figure S3. Multipoint model-based and non-parametric linkage analysis of Tunisian Arab-Berber LRRK2 p.G2019S families. A. Parametric linkage with divergent ages at onset (<56 or ≥ 56 years) , using an additive model with incomplete penetrance; B Parametric linkage hLOD cumulative scores; C. Non-parametric linkage D. Continuous trait analysis

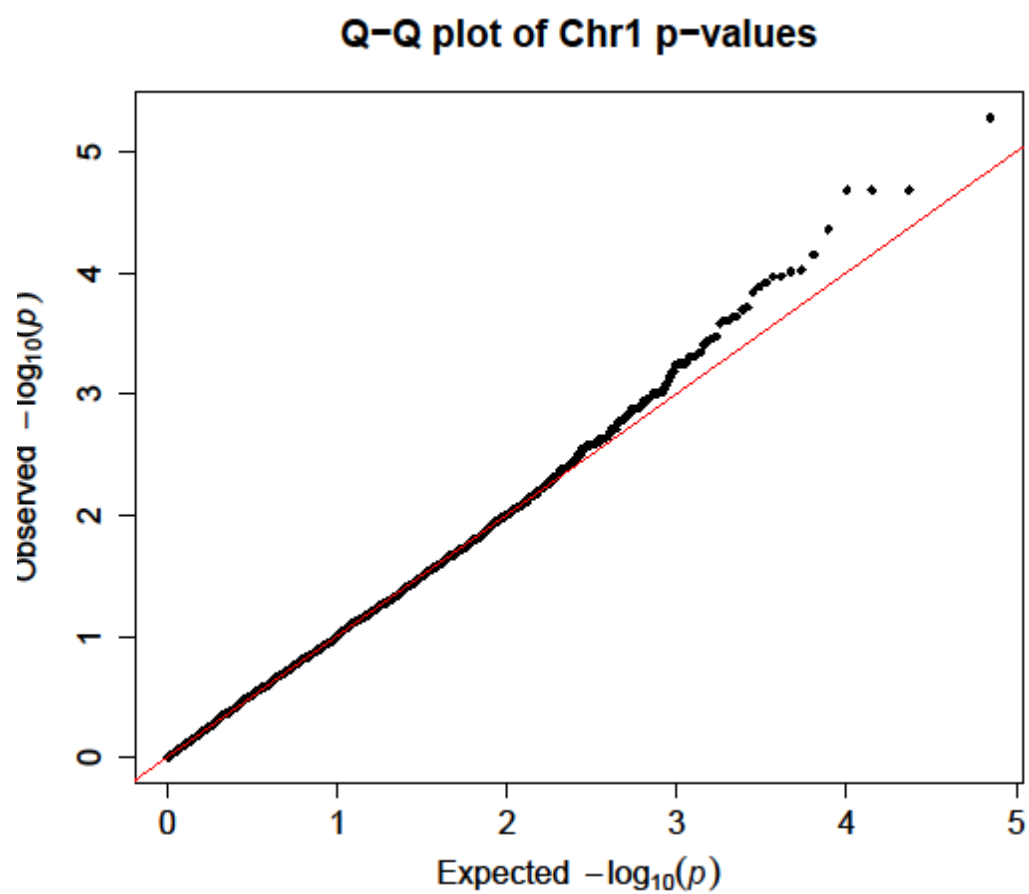


Figure S4. Chromosome 1 Q-Q plot values

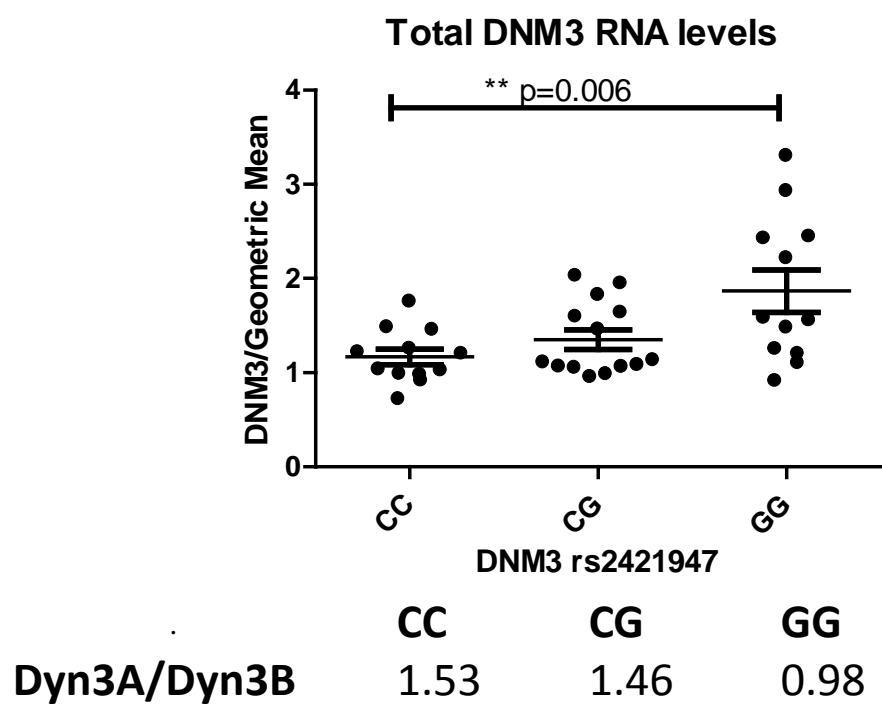


Figure S5. *DNM3* transcript levels normalized by geometric mean of housekeeping genes

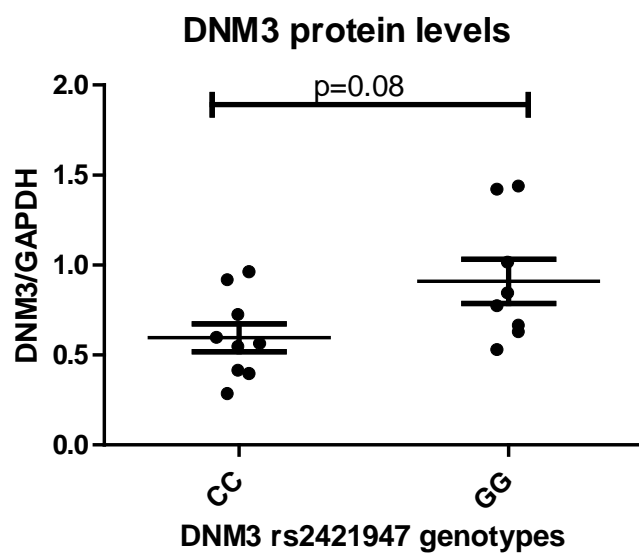


Figure S6. Dynamin 3 protein levels normalized by GAPDH

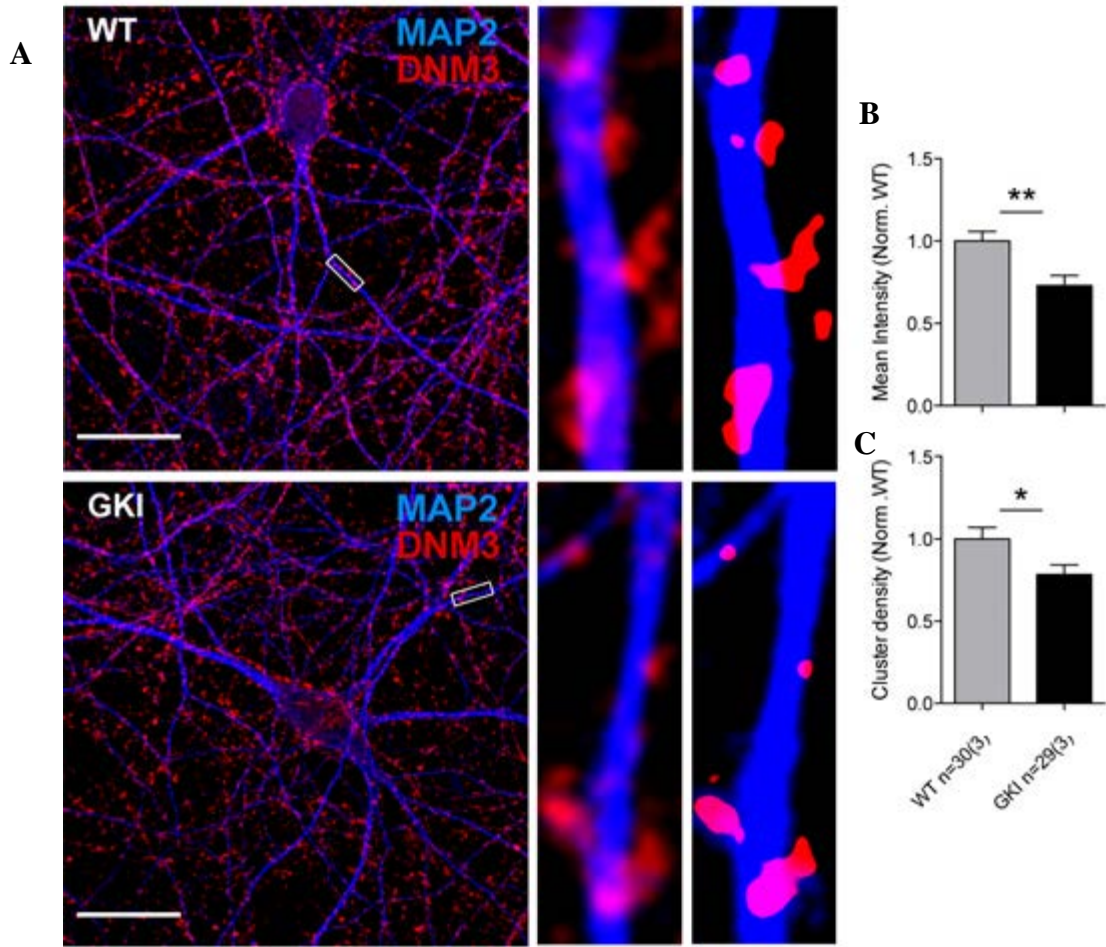


Figure S7. Dynamin 3 staining in cortical neurons

A. representative confocal microscopic images of dynamin-3 (red) and MAP2 (blue) staining in wild-type (WT) and GKI (LRRK2 p.G2019S) murine cortical neurons, cultured as previously described.⁴ Left: 60X 2-times zoom of individual neuron staining. Right: expanded region of interest with and without MAP2; B. Quantification of dynamin-3 intensity in cortical cultures (DIV=21). Scale bars, 50um, n=3 cultures per group; C. Quantification of dynamin-3 cluster density in cortical cultures (DIV=21) **= $p < 0.05$.

Supplementary references

1. Abecasis GR, Cherny SS, Cookson WO, Cardon LR. Merlin--rapid analysis of dense genetic maps using sparse gene flow trees. *Nature genetics* 2002; 30: 97-101.
2. Price AL, Patterson NJ, Plenge RM, Weinblatt ME, Shadick NA, Reich D. Principal components analysis corrects for stratification in genome-wide association studies. *Nature Genetics* 2006; 38, 904-909.
3. Cao H, Garcia F, McNiven MA. Differential distribution of dynamin isoforms in mammalian cells. *Molecular biology of the cell* 1998;9: 2595-609.
4. Beccano-Kelly DA, Kuhlmann N, Tatarnikov I, et al. Synaptic function is modulated by LRRK2 and glutamate release is increased in cortical neurons of G2019S LRRK2 knock-in mice. *Front Cell Neurosci* 2014;8:301.